08

The influence of metal oxide nanoparticles on the electrical characteristics of quasi-2D-graphene-nanotube films

© M.M. Slepchenkov,[1] P.V. Barkov,[1] S.G. Levitsky,[1] O.E. Glukhova[1,2]

[1] Saratov National Research State University,
410012 Saratov, Russia
[2] I.M. Sechenov First Moscow State Medical University,
119048 Moscow, Russia
e-mail: slepchenkovm@mail.ru

Received December 28, 2025
Revised December 28, 2025
Accepted December 28, 2025

Using density-functional tight-binding method, an *in silico* study of the energetic and electrical properties of hybrid quasi-2D carbon films with metal oxide nanoparticles on their surface was conducted. The hybrid carbon films are formed by covalently bonded graphene and single-walled nanotubes oriented vertically relative to the graphene plane. Titanium and hafnium oxides, which are strong dielectrics, are considered as metal oxides. The thermodynamic stability of the studied structures is estimated based on the binding energy. Electrical properties are assessed based on electrical resistance. The distribution of the Mulliken charge in the graphene–nanotube film + metal oxide system is analyzed.

Keywords: carbon films, density-functional tight-binding method, metal oxides, electrical resistance, partial charge.

DOI: 10.61011/TP.2026.05.63525.344-25

Introduction

One-dimensional carbon nanotubes (CNT) and two-dimensional graphene that are featuring outstanding structural, mechanical and physical properties [1,2], have attracted the attention of researchers for many years both from the standpoint of fundamental science and in terms of development of various technical applications based on these carbon nanomaterials, including supercapacitors, transistors, flexible and transparent electrodes, solar panels, devices with field emission [3]. Since late 2000s, attempts have been made to combine CNT and graphene to use the advantages of both carbon nanomaterials, creating a hybrid material characterized by improved properties due to their synergistic effect [4–15]. In the fully carbon nanomaterials, graphene should provide a platform with a large surface area for uniform distribution of CNT and the conductivity of the graphene-nanotube hybrid in the plane [14], while CNT should serve as a separator for graphene sheets, preventing their aggregation and ensuring the conductivity of the hybrid in the axial direction [15]. The variety of synthesis technologies used to produce hybrid carbon nanomaterials [13] allows to fabricate the graphene–nanotube architectures with different mutual arrangement and method of joining nanotube and graphene [16]. There are three main types of architecture of synthesized fully carbon nanomaterials based on CNT and graphene [16]. In the architecture of the first type, CNT are oriented parallel to the graphene plane, in the architecture of the second CNT they are oriented perpendicular to the graphene plane, and in the architecture of the third CNT they are wrapped in graphene. Graphene-nanotube materials with the architecture of the first two types are more common than the architecture of the third type and are widely studied both by computer modeling methods and by methods of physical experiment [17–24].

Graphene nanotube materials with a second type of architecture are more promising for a number of technical applications requiring low electrical resistance. As shown in [22], the contact resistance of a hybrid graphene-nanotube structure with CNT oriented perpendicular to the graphene plane is four times less than the contact resistance of a graphene-nanotube structure with CNT oriented parallel to the graphene plane. In addition, graphene-nanotube materials with architecture of the second type are considered promising materials for fabricating the thermally conductive interface materials [23,24]. In particular, it was shown in [23] that the use of graphene-CNT hybrids as a thermally conductive interface provided the nanocomposites containing aramid nanofibers with excellent photothermal transformation and Joule heating characteristics. The authors in [24] also demonstrated that hybrid all-carbon films with vertically oriented CNT had high longitudinal and transverse thermal conductivity due to additional conduction channels created by graphene in the transverse direction and nanotubes in the longitudinal direction. This study sheds light on the graphene–nanotube quasi-2D-films with vertically oriented single-walled CNT (SWCNT) seamlessly connected to graphene and metal oxide nanoparticles adsorbed on their surfaces. Nanoparticles of titanium oxide TiO_2 and hafnium oxide HfO_2 with pronounced dielectric properties are suggested as metal oxides. The predictive

analysis of the impact of type and concentration of metal oxide nanoparticles on the electronic and electrophysical properties of graphene-nanotube films is carried out using atomic modeling methods.

1. Research methods

To obtain atomistic models of hybrid carbon quasi-2D structures with a seamless connection of graphene and SWCNT, an original method of automated construction of atomic nets of seamless arbitrary shape joints of carbon nanostructures [25] was used. The construction method used includes geometric and dynamic stages. The geometric stage consists in building a triangulated nanonetwork that serves as an initial carcass for connecting the two considered carbon structures. During the dynamic stage, based on the geometry stage data, a seamless contact is formed between nanoobjects using the molecular dynamics (MD) method and the AIREBO [26] force field, which is the most suitable for describing carbon nanostructures. The time integration step was 0.1 fs. During MD modeling, normal conditions were applied (temperature 300 K and pressure of 10^5 Pa). To clarify the geometry of the supercell obtained using MD method and AIREBO force field, a double reoptimization of the atomic structure of selected versions of seamless graphene-SWCNT joints atomic nets was carried out using the self-consistent-charge density functional tight binding quantum method SCC DFTB [27]. The SCC DFTB method is chosen due to the polyatomic nature of the calculated supercells, which contain several hundred atoms. The optimization parameters were not only the coordinates of the atoms, but also the translation vectors L_x (along X axis), L_y (along Y axis) of the supercells of seamless joints. For a physically correct description of the interaction between carbon, hafnium, and oxygen atoms, the SCC DFTB method was additionally parameterized by creating a set of Slater-Koster (SK) parameters that defined the atomic orbitals of interacting atoms and their interaction energy. The parametrization matsci-0-3 [28] was used to delineate the interaction between carbon, titanium, and oxygen atoms.

The conductivity of the studied structures was analyzed within the framework of Landauer-Buttiker [29] formalism using the formula

$$G = 2e^2/h \int_{-\infty}^{\infty} T(E)F_T(E - E_F)dE, \qquad (1)$$

where the coefficient 2 before the integral takes into account the spin, $T(E)$ — averaged function of electron transmission, E_F — Fermi level of the electrodes, e^2/h — quantum of conductivity, F_T — function of thermal broadening of energy levels. Calculations of the conductivity characteristics were performed at a temperature of 300 K.

2. Results and discussion

The crystalline cells of the metal oxides TiO_2 and HfO_2 were taken from the international database Materials Project [30]. The crystal cells TiO_2 of tetragonal syngony with the spatial group $I4_1/amd$ and HfO_2 of monoclinic syngony with the spatial group $P2_1/c$ were selected for the analysis. The crystal section (001) was analyzed in both cases. The calculated supercell TiO_2 comprised 36 atoms (Fig. 1, a), supercell HfO_2 — comprised 44 atoms (Fig. 1, b). The supercell of the hybrid carbon film included SWCNT (16,0) with a height of 17.6 Å. The selected height of SWCNT is explained by the limitations imposed on the size of the calculated supercells by the quantum methods and approaches used. The supercell translation vectors along „zigzag“ and „armchair“ directions made 37.33 and 35.51 Å respectively.

The cases of adsorption of one, two, three, and four metal oxide nanoparticles on the surface of a hybrid carbon film were considered. The case with four nanoparticles corresponds to the maximum concentration considered, defined as the number of metal oxide particles per supercellular area. The location of metal oxide nanoparticles on the surface of the graphene-nanotube film was selected based on the results of optimization of the atomic structure of „graphene-nanotube film + metal oxide“system supercell. At that, for each of the considered cases of adsorption of metal oxide nanoparticles, the binding energy E_b was calculated, which was used to evaluate the thermodynamic stability of „graphene–nanotube film + metal oxide“ system. The bond energy was defined as the difference between the total energy of the graphene-nanotube film,+,metal oxide system and the total full energy of its component parts (graphene-SWCNT film and metal oxide nanoparticles). Figure 2 shows the equilibrium configurations of supercells of graphene-nanotube films with one (Fig. 2, a), two (Fig. 2, b), three (Fig. 2, c), and four (Fig. 2, d) nanoparticles TiO_2. Table 1 shows the energy and electrophysical characteristics of a graphene–nanotube film with a different number of nanoparticles TiO_2 on the surface.

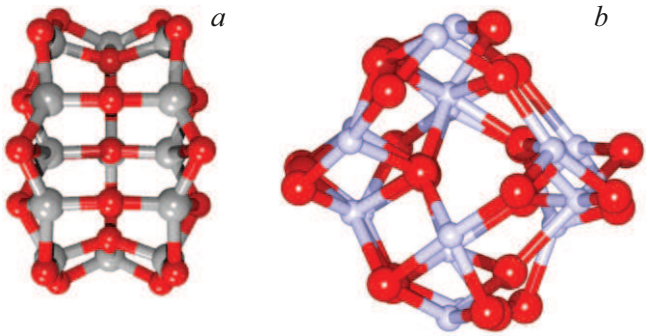

Figure 1. Crystalline supercells TiO_2 of tetragonal syngony with a spatial group $I4_1/amd$ (a) and HfO_2 of monoclinic syngony (b) with a spatial group $P2_1/c$.

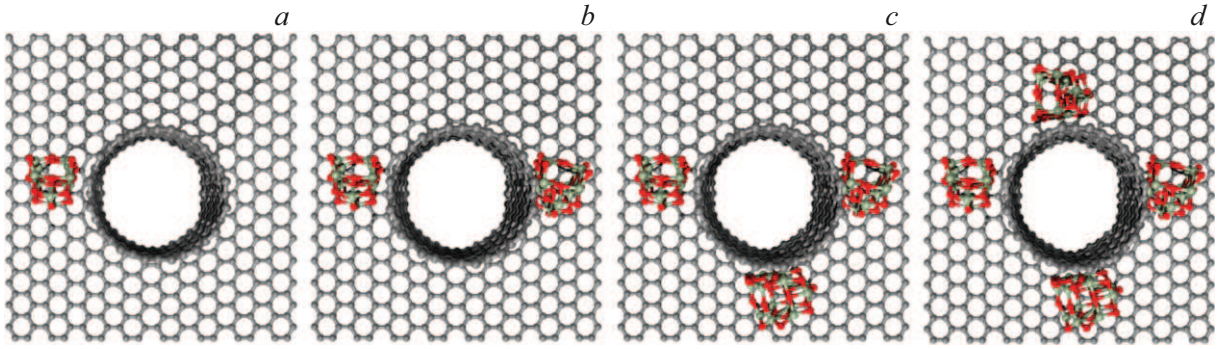

Figure 2. Equilibrium configurations of supercells of graphene-nanotube films with one (a), two (b), three (c) and four (d) nanoparticles TiO_2.

Table 1. Energy and electrophysical characteristics of the system „graphene–nanotube film + TiO_2“

Quantity of nanoparticles TiO_2	Energy of bond E_b, eV	Level Fermi E_F, eV	Resistance R, kΩ
1	−5.76	−4.84	58.6
2	−4.90	−4.69	27.6
3	−5.95	−4.60	22.4
4	−3.74	−4.52	19.2

It follows from the data in Table 1 that the bond energy E_b is negative in each of the considered cases of adsorption of nanoparticles TiO_2 and is in the range from −5.76 to −3.74 eV. Negative values of E_b indicate that the process of adsorption of TiO_2 nanoparticles on the surface of a graphene-nanotube film is energetically advantageous, and the resulting structural configurations of the system „graphene-nanotube film + TiO_2“ are distinguished by thermodynamic stability. It should be stressed that the adsorption of TiO_2 nanoparticles also impacted the change in the electronic structure of the graphene-nanotube film. Compared with the Fermi level position of the pure graphene–SWCNT (−5.05 eV) film the Fermi level of the system „graphene–nanotube film + TiO_2“ is shifted upwards along the energies axis reaching a point of −4.52 eV at maximum considered number of nanoparticles TiO_2. To explain the change in the Fermi level position of the graphene-SWCNT hybrid film during adsorption of TiO_2 nanoparticles, a Mulliken population analysis of electron orbitals was performed [31]. Fig. 3, illustrates the obtained distributions of the Mulliken (partial) charge over the atoms of the supercell of „graphene–nanotube film + TiO_2“ system with a different number of nanoparticles TiO_2. Analysis of the Mulliken (partial) charge distributions showed that in „graphene-nanotube film + TiO_2“ system, charge transfer from TiO_2 to the carbon carcass was observed, and with an increase in the number of TiO_2 nanoparticles, the value of the transferred charge grew from 1.5e to 4.7e (e — electron charge), reaching its maximum with four nanoparticles TiO_2. When graphene-SWCNT carbon film gets an additional charge it also affects the amount of resistance. If with one TiO_2 nanoparticle the resistance of graphene-nanotube film + TiO_2“ system is 58 kΩ, then with four TiO_2 nanoparticles it decreases threefold to 19.2 kΩ.

Similar research was carried out also for HfO_2 nanoparticles. Fig. 4 illustrates the equilibrium configurations of supercells of graphene–nanotube films with one (Fig. 4, a), two (Fig. 4, b), three (Fig. 4, c) and four (Fig. 4, d) nanoparticles HfO_2. Table 2 shows the energy and electrophysical characteristics of the graphene–nanotube film with a different number of nanoparticles HfO_2 on the surface. As can be seen from the data in Table 2, the supercells of graphene-nanotube films with different numbers of nanoparticles HfO_2 are characterized by negative values of bond energy E_b, and in their absolute value they are higher than the values E_b given in Table 1 for the cases of adsorption of nanoparticles TiO_2. The Fermi level of the graphene-SWCNT hybrid film (16,0) also shifts upward along the energy axis compared to its position when no metal oxides are available, as in the case of adsorption of TiO_2 nanoparticles, reaching the mark −4.11 eV with four nanoparticles HfO_2. The change in Fermi level position in the electronic structure of graphene-SWCNT (16,0) films in the presence of HfO_2 nanoparticles is explained by charge transfer in the „graphene-nanotube film + HfO_2“system, which flows from HfO_2 to the carbon carcass according to the Mulliken charge distributions shown in Fig. 5. The magnitude of the transferred charge rises from 2.3e to 7.7e (e — electron charge) with the growing number of HfO_2 nanoparticles.

The electrical resistance of the graphene-SWCNT carbon film (16,0) decreases with the addition of HfO_2 nanoparticles, as can be seen from the data in Table 2. When there are four nanoparticles of HfO_2 the resistance is about ∼ 9 kΩ, which is twice less than with four nanoparticles of TiO_2 and less than the resistance of pure graphene–SWCNT film of (16,0) (14.3 kΩ).

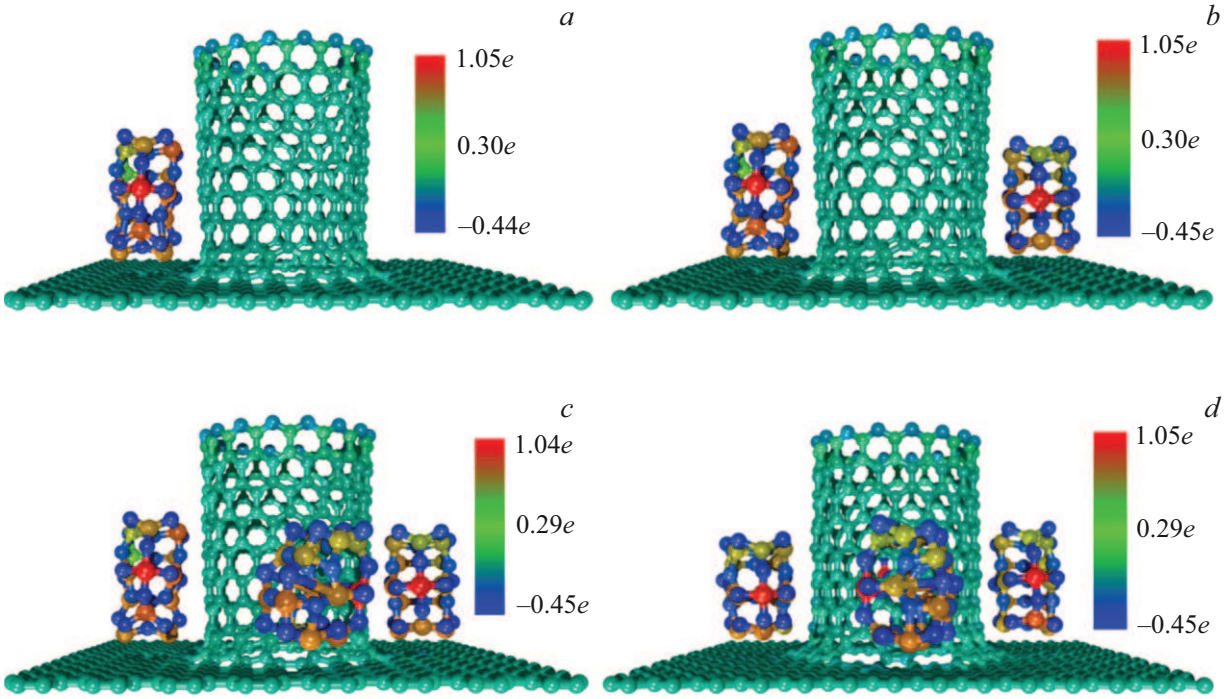

Figure 3. Distribution of the mulliken (partial) charge across the atoms of the supercell of „graphene–nanotube film + TiO_2“ system with one (*a*), two (*b*), three (*c*) and four (*d*) nanoparticles TiO_2.

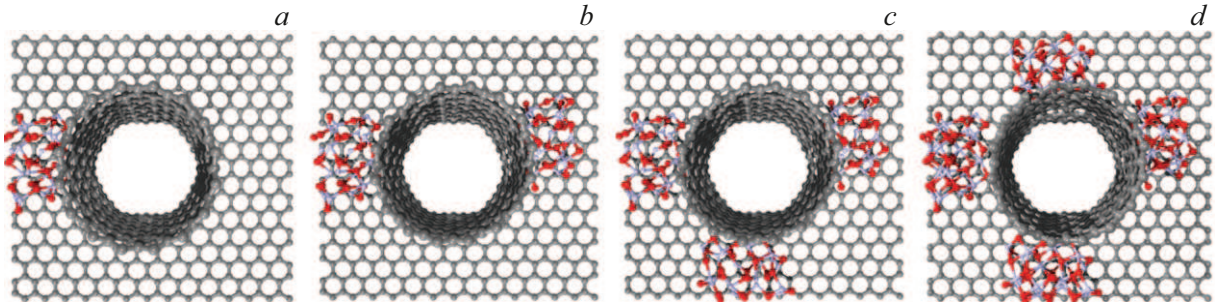

Figure 4. Equilibrium configurations of supercells of graphene-nanotube films with one (*a*), two (*b*), three (*c*) and four (*d*) nanoparticles HfO_2.

Table 2. Energy and electrophysical characteristics of the system „graphene–nanotube film + HfO_2“

Quantity of nanoparticles HfO_2	Energy of bond E_b, eV	Level Fermi E_F, eV	Resistance R, kΩ
1	−9.39	−4.86	28.2
2	−13.31	−4.58	24.5
3	−9.27	−4.29	16.1
4	−14.34	−4.11	8.6

To explain the observed effect of declining electrical resistance of the graphene-SWCNT (16,0) carbon film when its surface is functionalized with TiO_2 and HfO_2 nanoparticles, let us turn to the analysis of electron transmission function $T(E)$, which determines the number of conduction channels available for electron transport. For the pure graphene–SWCNT film (16,0) the value $T(E)$ is at Fermi level ~ 1.1. The smallest resistance ($\sim 9\,k\Omega$) of the graphene nanotube films functionalized with four nanoparticles of HfO_2 is explained by the fact that function $T(E)$ reaches its maximum at Fermi level (~ 1.9) among all the considered functionalizations. For a graphene-nanotube film functionalized with four TiO_2 nanoparticles with a resistance of 19.2 kΩ, the function $T(E)$ at Fermi level takes the value ~ 0.8. The difference in the values of function $T(E)$ of the graphene nanotube films functionalized with HfO_2 and TiO_2 (2.4) correlates well with the difference in the values of electrical resistance between them (2.2).

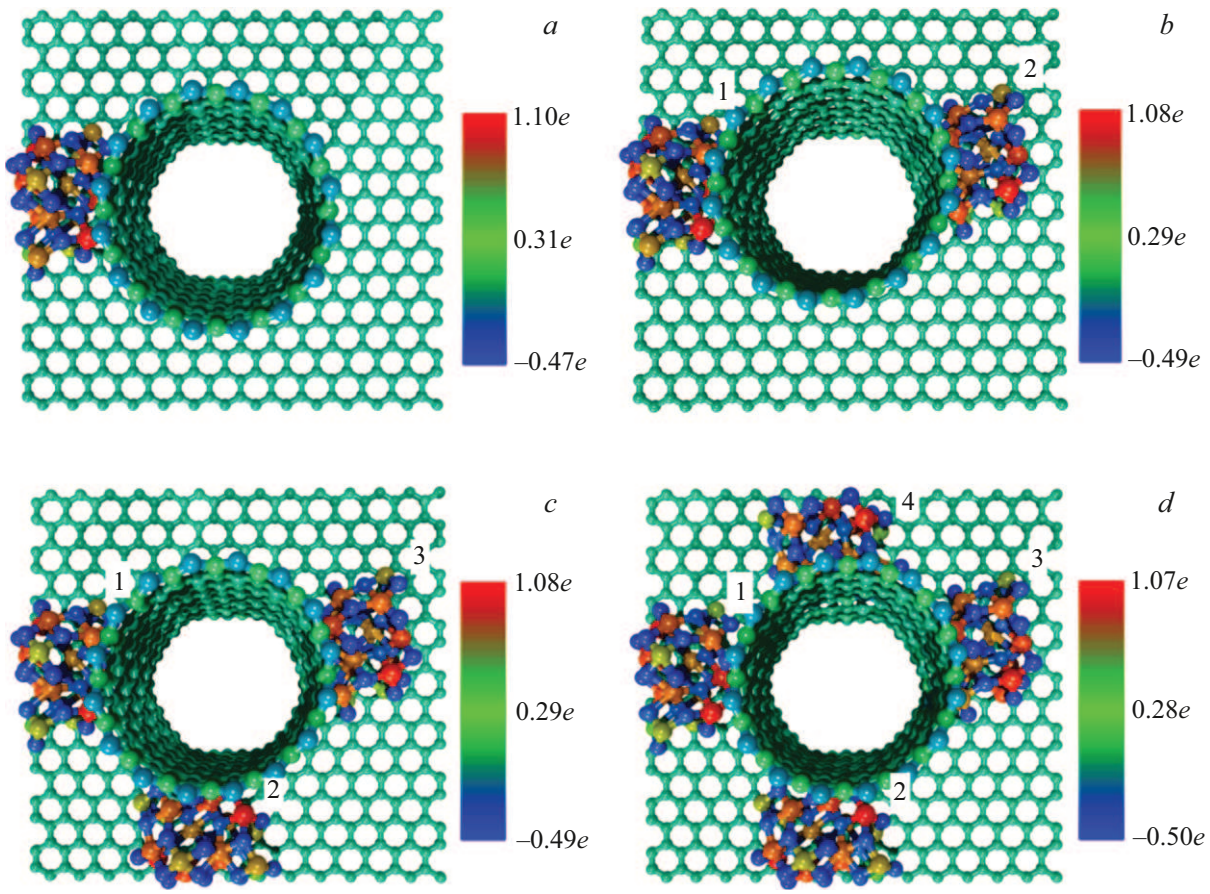

Figure 5. Distribution of the mulliken (partial) charge across the atoms of the supercell of „graphene–nanotube film + HfO_2“ system with one (*a*), two (*b*), three (*c*) and four (*d*) nanoparticles HfO_2.

The advantages HfO_2 over TiO_2 are related to the greater amount of partial charge transferred to the carbon carcass. In addition, in case of functionalization with four HfO_2 nanoparticles, the Fermi level of the graphene-SWCNT carbon film (16,0) (−4.11 eV) is significantly lower in modulus than in the case of functionalization with four TiO_2 nanoparticles (−4.52 eV). This proves that a hybrid carbon film functionalized with nanoparticles of HfO_2 is characterized by a larger valence band, which means that a larger number of valence electrons can pass into the conduction band, thereby creating better conditions for the current to flow.

Thus, based on the analysis, it can be concluded that the electrophysical characteristics of a hybrid graphene-nanotube film can be controlled by adsorption of metal oxide nanoparticles on its surface, varying the type and number of nanoparticles.

Conclusion

Based on the results of SCC DFTB calculations, patterns of influence of metal oxide nanoparticles (with TiO_2 and HfO_2 as an example) on the electrophysical properties of graphene-nanotube films with vertically oriented SWCNT (16,0), estimated by the magnitude of electrical resistance, were revealed. The presence of a charge transfer phenomenon in „graphene-nanotube film + metal oxide“ system in the direction from metal oxide nanoparticles to the carbon carcass has been established, resulting in a change in the electronic structure of the graphene-SWCNT hybrid film, accompanied by a shift in Fermi level upward along the energy axis, indicating an expansion of the valence band. The change in Fermi level position and charge transfer affect the electron transmission function, which determines the number of conduction channels available for current flow, and, as a result, the electrical resistance of the graphene-SWCNT film that declines with increasing number of metal oxide particles. When the graphene-nanotube film surface is functionalized with HfO_2 nanoparticles, the minimum resistance achieved is two times less than the minimum resistance achieved with TiO_2 nanoparticles which is explained by numerous conduction channels in case of HfO_2 and the greater amount of charge transferred by HfO_2 to the carbon carcass compared with nanoparticles of TiO_2. The examined graphene-nanotube films structures in the presence of metal oxide nanoparticles can be considered as a

promising nanomaterial for creating nanoelectronics devices, in particular, nanotransistors.

Funding

This study was supported by the grant from the Russian Science Foundation (project № 24-79-10316, https://rscf.ru/project/24-79-10316/).

Conflict of interest

The authors declare that they have no conflict of interest.

References

[1] V. Georgakilas, J.A. Perman, J. Tucek, R. Zboril. Chem. Rev., **115**, 4744 (2015) DOI: 10.1021/cr500304f
[2] O.S. Ayanda, A.O. Mmuoegbulam, O. Okezie, N.I. Durumin Iya, S.E. Mohammed, P.H. James, A.B. Muhammad, A.A. Unimke, S.A. Alim, S.M. Yahaya, A. Ojo, T.O. Adaramoye, S.K. Ekundayo, A. Abdullahi, H. Badamasi. J. Nanopart. Res., **26**, 106 (2024). DOI: 10.1007/s11051-024-06006-2
[3] D. Jariwala, V.K. Sangwan, L.J. Lauhon, T.J. Marks, M.C. Hersam. Chem. Soc. Rev., **42**, 2824 (2013). DOI: 10.1039/C2CS35335K
[4] R. Atif, F. Inam. Beilstein J. Nanotechnol., **7**, 1174 (2016). DOI: 10.3762/bjnano.7.109
[5] P.N. Nirmalraj, P.E. Lyons, S. De, J.N. Coleman, J.J. Boland. Nano Lett., **9**, 3890 (2009). DOI: 10.1021/nl9020914
[6] S. Nardecchia, D. Carriazo, M. C. Gutiérrez, M. L. Ferrer, F. del Monte. Chem. Soc. Rev., **42**, 794 (2013). DOI: 10.1039/C2CS35353A
[7] C.-Y. Lin, Z. Zhao, J. Niu, Z. Xia, Synthesis. J. Phys. D Appl. Phys., **49**, 443001 (2016). DOI: 10.1088/0022-3727/49/44/443001
[8] M.M. Slepchenkov, P.V. Barkov, D.A. Kolosov, O.E. Glukhova. C, **9** (2), 51 (2023). DOI: 10.3390/c9020051
[9] A. Gbaguidi, S. Namilae, D. Kim. Nanotechnology, **31**, 255704 (2020). DOI: 10.1088/1361-6528/ab7fcc
[10] X. Zhao, L. Qiu, D. Kong, Y. Huang, J. Liu. Materials, **16**, 6571 (2023). DOI: 10.3390/ma16196571
[11] M.R. Zakaria, M.F. Omar, M.S. Zainol Abidin, H. Md Akil, M.M.A.B. Abdullah. Compos. -A: Appl. Sci. Manuf., **154**, 106756 (2022). DOI: 10.1016/j.compositesa.2021.106756
[12] S. Pyo, Y. Eun, J. Sim, K. Kim, J. Choi. Micro Nano Syst. Lett., **10**, 9 (2022). DOI: 10.1186/s40486-022-00151-w
[13] V.T. Dang, D.D. Nguyen, T.T. Cao, P.H. Le, D.L. Tran, N.M. Phan, V.C. Nguyen. Adv. Nat. Sci.: Nanosci. Nanotechnol., **7**, 033002 (2016). DOI: 10.1088/2043-6262/7/3/033002
[14] X. Wu, F. Mu, H. Zhao. J. Mater. Sci. Technol., **55**, 16 (2020). DOI: 10.1016/j.jmst.2019.05.063
[15] W. Du, Z. Ahmed, Q. Wang, C. Yu, Z. Feng, G. Li, M. Zhang, C. Zhou, R. Senegor, C.Y. Yang. 2D Mater., **6**, 042005 (2019). DOI: 10.1088/2053-1583/ab41d3
[16] B. Liu, J. Sun, J. Zhao, X. Yun. Adv. Compos. Hybrid Mater., **8**, 1 (2025). DOI: 10.1007/s42114-024-01074-3
[17] J. Sheng, Z. Han, G. Jia, S. Zhu, Y. Xu, X. Zhang, Y. Yao, Y. Li. Adv. Funct. Mater., **33**, 2306785 (2023). DOI: 10.1002/adfm.202306785
[18] C. Le, X. Xudong, L. Mengya, L. Hao, Z. Xiahong, Y. Gui. APL Mater., **9**, 041110 (2021). DOI: 10.1063/5.0045100
[19] Z. Li, Z.H. Li, Y. Zhang, X. Xu, Y. Cheng, Y. Zhang, J. Zhao, N. Wei. ACS Sens., **9**, 2499 (2024). DOI: 10.1021/acssensors.4c00170
[20] Y. Li, Q. Ai, L. Mao, T. Gong, Y. Lin, G. Wu, W. Huang, X. Zhang. Sci. Rep., **11**, 21006 (2021). DOI: 10.1038/s41598-021-00307-5
[21] T. Xu, J. Jiang. Phys. Chem. Chem. Phys., **25**, 5066 (2023). DOI: 10.1039/D2CP04797G
[22] M. Gao, Z.L. Huang, B. Zeng, T.S. Pan, Y. Zhang, H.B. Peng, Y. Lin. Appl. Phys. Lett., **106**, 051601 (2015). DOI: 10.1063/1.4907642
[23] M. Lan, X. Jia, R. Tian, L. Feng, D. Shao, H. Song. Carbon, **219**, 118850 (2024). DOI: 10.1016/j.carbon.2024.118850
[24] K. Xiong, C. Ma, J. Wang, X. Ge, W. Qiao, L. Ling. Ceram. Int., **49**, 8847 (2023). DOI: 10.1016/j.ceramint.2022.11.039.
[25] G. Zhang, O.E. Glukhova. Comput. Mater. Sci., **184**, 109943 (2020). DOI: 10.1016/j.commatsci.2020.109943
[26] A. Van Duin, S. Dasgupta, F. Lorant, W.A. Goddard III. J. Phys. Chem. A, **105**, 9396 (2001). DOI: 10.1021/jp004368u
[27] M. Elstner, D. Porezag, G. Jungnickel, J. Elsner, M. Haugk, Th. Frauenheim, S. Suhai, G. Seifert. Phys. Rev. B, **58**, 7260 (1998). DOI: 10.1103/PhysRevB.58.7260
[28] DFTB+. Available online: https://dftbplus.org/ (accessed on 1 February 2024)
[29] S. Datta. *Quantum Transport: Atom to Transistor* (Cambridge University Press: Cambridge, London, UK, 2005), p. 404.
[30] *Materials Project Available online*: https://nextgen.materialsproject.org/ (accessed on 1 February 2024)
[31] R.S. Mulliken. J. Chem. Phys., **23**, 1833 (1955).

Translated by T.Zorina